An Advanced Weather Surveillance Processor for Airport Surveillance Radars*

Mark E. Weber
M.I.T. Lincoln Laboratory
244 Wood Street
Lexington, Massachusetts 02173-9108

Thomas A. Kays
Federal Aviation Administration
1825 Connecticut Avenue, SW
Washington, DC 20009-5708

1. INTRODUCTION

This paper describes an enhanced weather processor for the Federal Aviation Administration's Airport Surveillance Radar (ASR-9) that will include Doppler wind estimation for the detection of low altitude wind shear, scan-to-scan tracking to provide estimates of the speed and direction of storm movement and suppression of spurious weather reports currently generated by the ASR-9's six-level weather channel during episodes of anomalous radar energy propagation (AP). This ASR-9 Wind Shear Processor (WSP) will be implemented as a retrofit to the ASR-9 through the addition of interfaces, receiving chain hardware and high-speed digital processing and display equipment.

Thunderstorm activity in terminal airspace (the volume extending approximately 30 nmi from an airport and to 15,000 feet altitude) is an obvious safety issue and makes a significant overall contribution to delay in the United States commercial aviation industry. Associated low-altitude wind shear has been identified as the primary cause of a number of air carrier accidents, involving almost 600 fatalities. Correlations of aircraft arrival and takeoff delay with associated weather conditions suggest that thunderstorm activity may account for 40 to 50 percent of serious delay within the United States [1].

The WSP modification to the ASR-9 will provide the functional capabilities of the Terminal Doppler Weather Radar (TDWR) at airports whose operation levels and/or thunderstorm exposures do not justify the costs of the dedicated radar. Field testing of a prototype version of the ASR-9 WSP has confirmed that the weather information products it generates are accurate and are operationally useful in an Air Traffic Control (ATC) environment.

2. TECHNICAL DESCRIPTION

A. Low Altitude Wind Shear Phenomena

Microbursts occur when intense, small-scale downdrafts from thunderstorms reach the earth's surface and diverge horizontally in a roughly cylindrically symmetric pattern. Aircraft penetrating the resulting surface wind outflow encounter a dangerous headwind to tailwind velocity transition (i.e., loss of airspeed), exacerbated by the downdraft in the microburst core. Microburst onset times may be extremely short, with the divergent outflow reaching peak intensity within a few minutes of the downdraft first reaching the surface.

Gust fronts are thunderstorm outflows whose leading edges propagate away from the generating precipitation, creating a convergent wind shear along their leading edge. Because the wind shear encountered by an aircraft penetrating a gust front increases the plane's lift, a gust front is less hazardous than the wind shear associated with a microburst. The winds behind a gust front, however, are turbulent, and the long-term change of wind direction following passage of the front affects runway operations. Tracking and predicting gust front arrivals before they reach an airport allows for more efficient use of runways.

B. ASR-9 Parameters

The ASR-9 operates at 11 cm wavelength, transmitting uncoded, 1.1 MW, one-microsecond pulses with linear vertical or right-hand circular polarization. The radar's beam is relatively narrow in azimuth (1.4 degrees) but utilizes broad, cosecant-squared elevation patterns (5 degree half-power beamwidth) to detect aircraft from the surface to approximately 20,000 feet. "High" and "low" elevation beams are employed in a range-azimuth gated (RAG) mode to reduce ground clutter illumination at short range. The antenna is scanned in azimuth at a rate of 12.5 RPM. The radar's pulse repetition frequency (PRF) is varied in a block-staggered mode about its average value (approximately 1000 per second) to mitigate "blind speeds" for aircraft; during the time period that the antenna sweeps through one beamwidth in azimuth, eight pulses are transmitted at a lower PRF followed by 10 pulses transmitted at a PRF that is 9/7 times higher.

The parameters of the Airport Surveillance Radar presented formidable challenges for development of the WSP. The radar's rapid scan rate and variable PRF waveform precluded the use of conventional ground clutter filter designs and "pulse-pair" or fast Fourier Transform (FFT) based weather spectrum moment estimation. Accurate measurement of microburst outflow winds -- a phenomenon confined to the lowest 100-500 m of the atmosphere -- is complicated by the contamination of the outflow Doppler signal by echoes from precipitation aloft entering the broad surveillance beam at higher elevation angle. These interfering signals are normally at a markedly different Doppler velocity than the outflow and will prevent accurate measurement of the near-surface radial wind velocity if conventional mean-velocity estimators are employed. Gust fronts and "dry" microbursts (divergent outflows associated with little or no rain at the surface) produce signals that are often near the system noise level and may be fragmented by ground clutter, second-trip weather echoes and other forms of interference.

C. WSP Interfaces to the ASR-9

The WSP is an "outboard" processing add-on to the ASR-9 that must not adversely effect the radar's fundamental mission of aircraft detection and tracking. Extraction of necessary signals is accomplished in a manner that does not increase the overall noise figure or decrease the dynamic range of the ASR-9's target channel.

As discussed below, accurate microburst outflow wind measurement requires processing of data acquired nearly simultaneously from the ASR-9's high and low elevation beams. When the radar operates in linear polarization, this is accomplished

* This work was sponsored by the Federal Aviation Administration. The views expressed are those of the authors and do not reflect the official policy or position of the U.S. Government.

through addition of switches and couplers in the existing RF waveguide paths. In the range interval of operational concern for low-altitude wind shear detection (0-15 nmi), the existing RAG beam switch connects the target channel to the high elevation beam signal so as to reduce the level of ground clutter. The unused low beam signal is shunted to the wind shear processor's receiving chain via an added switch that is slaved to the target processor's RAG circuit. High beam signals for the WSP are extracted simultaneously from a 3 dB coupler inserted in front of the existing beam switch. The resulting loss of high beam signal power to the target channel is compensated for by appropriately reducing the sensitivity time control (STC) attenuation used at these short ranges. When the radar operates in circular polarization mode, weather signals are derived from separate antenna ports that provide the opposite-sense circularly polarized signal component. High and low beam signals for the WSP are acquired on alternating scans of the antenna without impact on the target channel.

The WSP receivers are double-conversion receivers with digital automatic gain control in the IF stage and quadrature video detectors providing baseband output. The stable local oscillator and coherent local oscillator signals are tapped from the ASR-9 and are isolated from the radar by circulators. In combination with 14 bit A/D converters, the AGC receiver provides 129 dB total system dynamic range. This wide dynamic range is critical in detecting low cross section weather phenomena in the presence of strong ground clutter.

D. Digital Processing Computers

In our prototype system, the signal processing computer operates as a loosely coupled multi-processor, incorporating several single-board computing systems connected by VME busses. A data input processor receives the I and Q samples and distributes these to six array processing boards. Each board performs the full suite of high-speed arithmetic operations necessary for ground clutter suppression and weather parameter estimation on a specific interval of range gates. The resulting "base data" (reflectivity, radial velocity and spectrum width estimates) are reassembled by an output processor and passed on to the meteorological detection algorithms.

For convenience, microburst and gust front detection, storm motion estimation and the suppression ground clutter breakthrough during anomalous propagation conditions are accomplished using UNIX workstations connected to the signal processing computer via an Ethernet local area network (LAN). In a production implementation of the WSP, these outboard workstations would be replaced by additional single-board computers in order to minimize processor size and expense.

E. Data Processing Algorithms

Multi-PRF Coherent Processing for Clutter Suppression and Periodogram or Autocorrelation Function Estimation: The ASR-9's block-staggered signaling waveform does not provide a sufficient number of consecutive pulses at the same PRF to attain the Doppler resolution necessary for ground clutter suppression and estimation of low-altitude radial wind velocity. For the WSP, we utilize an "extended coherent processing interval" consisting of three successive pulse-blocks -- eight low PRF pulses, 10 high PRF pulses and the following eight pulse low PRF block. High-pass filters for suppression of ground clutter are shift-variant, non-causal finite impulse response filters that can be designed to achieve Chebyshev or mean-squared error optimality while maximizing the number of output pulses available for velocity estimation [2]. The filter group-delays are controlled so as to provide output sample time spacing equal to that of the input. Theoretical suppression of scan-modulated ground clutter in excess of 60 dB is readily achievable with these designs; transmitter/receiver chain instability limits realizable suppression to approximately 45 dB.

In order to approximately match the clutter filter transfer functions to the inverse of the scan modulated ground clutter, plus noise spectrum, one of four filters is selected based on the intensity of the clutter and weather in each resolution cell [3]. The filter transfer functions vary from all-pass to a deep stop-band that yields 60 dB clutter suppression (ignoring the limiting effect of transmitter/receiver chain instability). A "Clear Day Map," storing clutter residue power for each of the four filters for each resolution cell, is used to select the least attenuating filter that produces an output weather-to-clutter-residue ratio in excess of a threshold (nominally 10 dB). This procedure minimizes distortion of the weather echo spectrum in the filtering process, thereby reducing associated biases in reflectivity or radial velocity estimates.

Algorithms for estimation of the low-altitude component of the radial wind field require that signals from the high and low receiving beams be represented in terms of either their autocorrelation functions or amplitude and phase spectra. Generation of these functions in a manner that properly accounts for the non-equal spacing of the time samples is accomplished via a second, shift-variant linear operation. Essentially, this implements a generalized Discrete Fourier Transform (DFT) by fitting, through a pseudo-inverse matrix operator, the available non-equispaced time samples to a sum of harmonically spaced sinusoids. Equispaced time samples for computation of autocorrelation function estimates, if desired, can be obtained by cascading this operator with a conventional inverse DFT. As described in an accompanying paper in these proceedings [4], the coherent processing over multiple PRFs provides the benefit of resolving velocity ambiguities.

Low Altitude Radial Velocity Estimation: Except at very short range (2 km or less), the fan-shaped elevation beam of an ASR-9 results in the reception of energy scattered from an altitude interval that is large compared to the depth of a microburst outflow. Detection and intensity characterization for microburst-induced low altitude wind shear requires that interfering signal components associated with these scatterers aloft be rejected in the velocity estimation process since their Doppler velocity normally differs markedly from that of winds in the outflow.

Discrimination between spectral components scattered from the low altitude thunderstorm outflow and those produced by winds aloft can be performed by comparing signals received simultaneously in an ASR's high and low receiving beams. Figure 1 shows that the elevation gain patterns of these beams differ significantly at angles below 5 degrees, with the difference increasing monotonically towards the horizon. Examples of measured power spectra in microburst outflows (first and third rows of Figure 2) indicate that this gain pattern difference is reflected in the high-low beam relative amplitudes of signal components associated with near surface scattering. For such signal components, the power spectrum density (PSD) of low-beam signals significantly exceeds that of high-beam signals; this contrasts markedly with interfering energy scattered from higher elevation angles where the high beam PSD equals or exceeds the low beam PSD.

A computationally efficient algorithm for exploiting this relationship utilizes parametric modeling of the received high and low beam power spectra [5]. Consistent with many of the measured spectra, the power spectrum of ASR weather signals is modeled as the summation of two Gaussian-shaped components -- one corresponding to scattering from near the earth's surface and a second representing interfering signal components scattered from aloft. The unknown amplitudes, center frequencies and widths of these Gaussian components can be obtained from estimates of the high and low beam autocorrelation functions at delays of zero to two times the average radar pulse repetition interval. The center frequency of the desired low-altitude Gaussian spectrum component

yields the desired near surface radial velocity. The second and fourth rows of Figure 2 show the parametrically modeled spectra and low altitude radial velocity estimates that correspond to the measurements in the first and third rows. It is seen that the algorithm retrieves the near surface radial velocity component accurately in spite of the wide intrinsic width of the ASR's weather echo spectra.

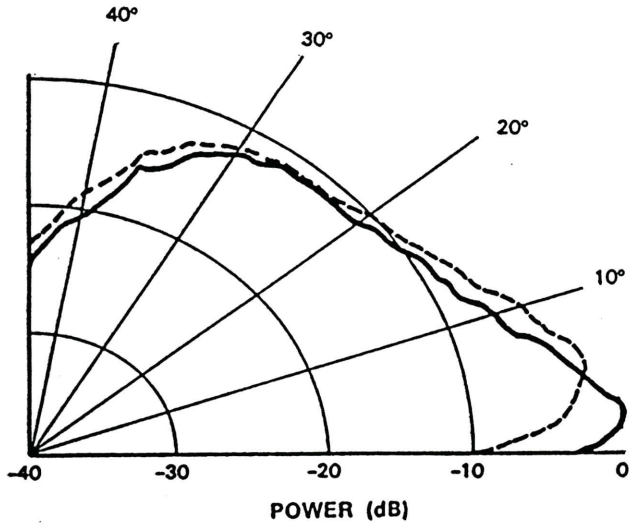

Figure 1. ASR-9 elevation beam patterns. Low and high beams plotted with solid and dashed lines, respectively.

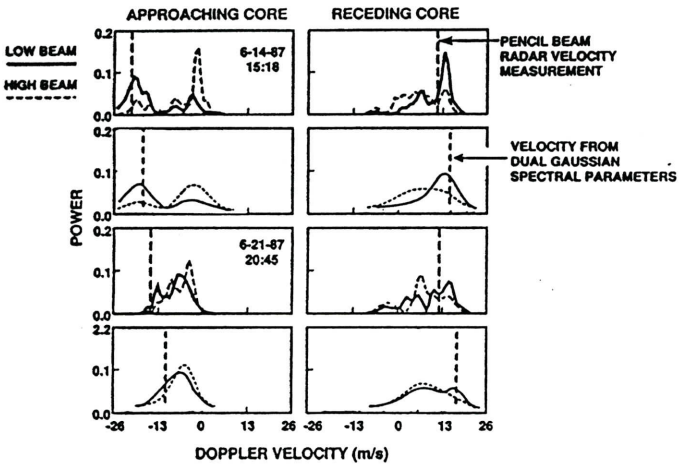

Figure 2. First and third rows show ASR testbed power spectrum measurements from radar resolution cells in the approaching and receding velocity cores of example microbursts. Second and fourth rows are corresponding spectra and velocity estimates reconstructed using the dual Gaussian parametric model described in the text.

Reflectivity and Spectrum Width Estimation: The precipitation equivalent reflectivity factor Z_e is estimated using the computed signal autocorrelation function at zero-delay, after subtracting a stored estimate for the system noise level. Data from the high receiving beam are used for the reflectivity estimates out to a range of approximately 5 km; low beam data are used at greater ranges where ground clutter interference is less severe.

Weather echo spectrum width is calculated using a weighted, quadratic regression to the logarithms of the magnitudes of the signal autocorrelation function estimated at lags 0 through 4 times the average pulse repetition interval (PRI). This estimator is based on an assumption that the echo power spectra are approximately Gaussian in shape.

Microburst Detection Algorithm: The microburst detection algorithm is a two-stage process. A "front-end" searches for candidate divergence signatures in the Doppler velocity field using a straightforward radial by radial search for the characteristic increasing (with range) velocity signature associated with microburst outflows. The resulting "shear segments" are then subjected to scan-to-scan continuity tests, grouped azimuthally and passed on to a "verification process" that ensures that the candidate microburst detections are physically plausible.

The verification process incorporates image processing and expert system components to:

- Determine whether the temporal and spatial evolution of the reflectivity (i.e., liquid water) field associated with Doppler divergence signatures is physically consistent with the processes that give rise to microburst outflows;
- Identify Doppler divergence features that are likely not to be associated with hazardous microburst outflows. An example of such a feature includes bending of the "zero-isoDoppler line" as a result of changes of wind direction with altitude. The "zero-isoDoppler line" is a roughly radially oriented line at the azimuth at which the wind vector is at right angles to the radar beam. When this line bends with increasing range as the radar beam rises in altitude, radial divergence may be detected although no microbursts are present;
- Characterize the strengths, areas, motions and symmetries of the candidate Doppler divergence signatures. In aggregate, these attributes serve as reliable discriminants between valid microburst outflow signatures and false-alarms that result from ground clutter breakthrough, unusual vertical distributions of precipitation reflectivity and/or radial velocity, and artifacts associated with storms whose translational velocities are large.

Gust Front Detection Algorithm: The WSP's "Machine Intelligent" Gust Front Detection Algorithm (MIGFA) [6] exploits image processing/expert system technology developed at Lincoln Laboratory originally in the context of Automatic Target Recognition [7]. MIGFA employs multiple, independent "functional template correlators" that search the WSP's reflectivity and Doppler velocity imagery for features that are selectively indicative of gust fronts. Because the ASR-9's intrinsic sensitivity is often inadequate to directly measure the convergent radial velocity pattern associated with gust fronts, MIGFA's feature detectors are designed to recognize manifestations of the "thin line echo" along a front's leading edge. This subtle feature can be recognized as slight enhancement in radar reflectivity relative to background and/or as a line of spatially coherent Doppler velocity estimates embedded in a background where the gate-to-gate estimate variance is much higher. Movement of thin lines, through a background of stationary ground clutter residue and slower moving storm cells aids in their identification.

The outputs of the feature detectors are expressed as interest images, whose values (0 to 1) specify the degree of evidence that a gust front is present. The multiple interest images are fused to form an overall map of evidence indicating the locations of possible gust fronts. From this image, fronts are extracted as chains of points

("events") and correlated with prior events by establishing a point-to-point correspondence. Heuristics are applied to reject chain points whose apparent motion is improbable. The history of scan-to-scan event correspondences is then used to make predictions of where points along the front will be at future times. This prediction serves both as an operational product for planning of gust front arrivals at an airport, and as an input to an "ANTICIPATION" interest image that serves to heighten MIGFA's sensitivity where fronts are expected to be.

Storm Motion Algorithm: The storm motion algorithm uses scan-to-scan correlation of the WSP's reflectivity measurements to estimate the speed and direction of storm advection. Reflectivity images are thresholded to produce binary representations of storm cells. These are partitioned into "correlation boxes" (typically 10 km x 10 km). For each box, a scan-to-scan displacement vector is computed by finding that displacement vector which maximizes the cross correlation between scans N and N-1. The uniform grid of displacement vectors so derived is smoothed spatially (nine-point median filter) and temporally (single-pole recursive filter). The final stage of processing is an analysis of the original reflectivity image to identify local reflectivity maxima corresponding to distinct storm cells. The closest gridded displacement vector is used to estimate the speed and direction of storm motion for each identified cell.

Censoring of Ground Clutter Breakthrough Caused by Anomalous Propagation: Anomalous propagation conditions result in ground clutter that is more intense than the values stored in the signal processor's Clear Day Map. When this occurs, the adaptive filter selection process described above may result in inadequate clutter suppression so that the reflectivity and Doppler velocity estimates are contaminated by low-Doppler energy from the ground clutter. This condition is flagged by testing the mean Doppler and spectrum width of the (post clutter filtered) signal to discriminate between true weather echoes and AP-induced clutter breakthrough. While precipitation echoes may have a low mean Doppler velocity (for example, when moving tangentially to the radar's beam) their spectrum width is almost always significantly broader than that of the antenna scan modulated ground clutter owing to turbulence and vertical shear within the altitude interval spanned by the ASR-9's fan beam. The AP-censor flag is set "true" in resolution cells where signal spectrum width is less than 2 m/s and the mean Doppler velocity is less than 1 m/s. After spatial filtering to remove remaining "speckle" breakthrough, the censor flag map is used to prevent erroneous precipitation indications from appearing on the operational displays, and as data quality information for the meteorological detection algorithms.

F. Operational Displays

The WSP provides graphical and alphanumeric displays for use by Air Traffic controllers and their supervisors. The displays and operational procedures are largely the same as those developed for the TDWR.

The Geographic Situation Display (GSD) illustrated in Figure 3 provides broad-area, weather situational awareness and is intended primarily for supervisor usage as an aid to traffic management. The GSD presents graphical representations of the location and intensity of precipitation, microbursts and gust fronts, as well as estimates of the speed and direction of motion for precipitation cells and gust fronts. An estimate of the wind vector behind gust fronts allows for anticipation of runway changes that will be necessary following gust front passage. When wind shear events intersect active runways or approach departure corridors, runway specific alphanumeric messages are generated on the "ribbon" displays. These are read off without interpretation by the local controller to pilots as planes are cleared for landing or takeoff.

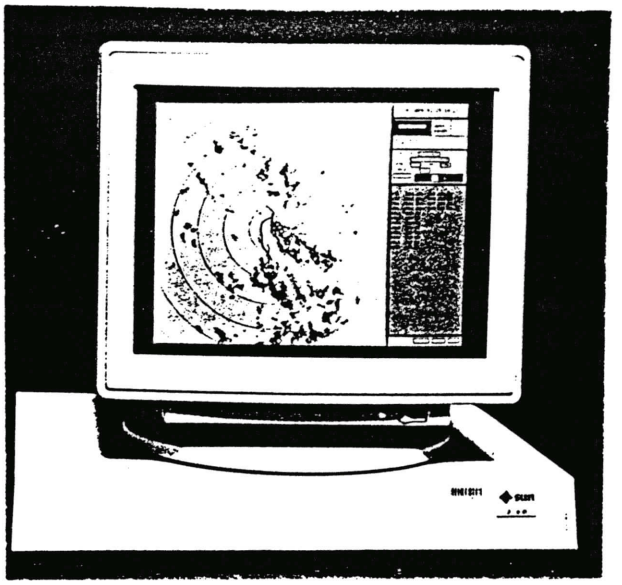

Figure 3. Geographic Situation Display.

3. FIELD EVALUATION PROGRAM

A. WSP Testbed Chronology

An experimental Airport Surveillance Radar facility has supported weather data collection for use in development and validation of the WSP's signal processing and meteorological detection algorithms and operational demonstration of WSP products at actual Air Traffic Control towers.

The testbed was established in 1987 in Huntsville, AL. using an ASR-8 modified to emulate an ASR-9 in terms of transmitted signal waveform and system stability. Convective activity in Huntsville is primarily airmass during summer months, with a transition to more organized squall lines and frontal storms during the fall, winter and spring. In 1989 the testbed was moved to Kansas City, KS to investigate algorithmic performance in an environment subject to highly organized severe weather systems characteristic of the Midwest. From 1990 to 1992 the testbed was operated at Orlando, FL. The central Florida peninsula experiences the highest frequency of thunderstorm activity within the continental U.S. The testbed's ASR-8 was replaced by a production ASR-9 during the Orlando field program and operational testing of the weather products in the Orlando ATC facility commenced. In 1993 the testbed was moved to Albuquerque, NM to support refinement of algorithms for operation in an environment subject to frequent "dry" wind shear activity, extreme ground clutter and rapid changes in the ambient wind's speed and direction with altitude.

At each site, one or more pencil-beam Doppler weather radars and an anemometer network have been operated to provide the meteorological "truth" data necessary for development and validation of the WSP's algorithms.

B. Technical Performance

The performance of the WSP's microburst and gust front detection algorithms have been quantified using the metrics Probability of Detection (P_d) and Probability of False-Alarm (P_{fa}). These are derived by "scoring," on a scan-by-scan basis, the output of the WSP's meteorological detection algorithms against time-coincident truth. This is generated through manual inspection of the data derived from the supporting sensors described above. The P_d is

therefore a scan-by-scan measure of the probability that the WSP will alert when wind shear is actually present. Likewise, P_{fa} is the scan-by-scan probability that a WSP alert will not correspond to actual wind shear exceeding the threshold for alert declaration (20 kts loss in the case of a microburst, 15 kts gain in the case of a gust front).

Table 1 lists these performance statistics for the microburst detection algorithm. The statistics are shown for the last four years when the WSP products have been used operationally. Data collected prior to that period were used in development of the microburst detection algorithm but have not been carefully "scored" with the current version.

Table 1.
Microburst algorithm detection and false alarm probabilities by year.

	Orlando			Albuquerque
	'90	'91	'92	'93
P_d	0.97	0.98	0.98	0.86
P_{fa}	0.10	0.08	0.10	0.18

In Orlando, the detection probabilities significantly exceeded the TDWR System Requirement of 0.90. False-alarm probabilities were likewise maintained at the corresponding P_{fa} requirement of 0.10 or less. The Albuquerque site presented a significantly more challenging environment for radar detection of microbursts. Severe ground clutter, fast moving storms and significant variation in ambient wind speed and direction with altitude complicate the detection of actual microburst signatures and increase the probability that the WSP's estimated low-altitude radial velocity field will exhibit erroneous divergence signatures.

The Albuquerque statistics reflect aggressive filtering of candidate divergence signatures using the "verification" module described above to achieve an operationally acceptable P_d and P_{fa}. Although somewhat outside the stated TDWR performance requirements, the achieved accuracy for the microburst detection function was viewed very favorably by the Albuquerque Air Traffic Controllers who used the product operationally.

Gust front detection statistics are shown in Table 2 for the years where MIGFA has been tested. These are very positive for the moist southeast U.S. environment represented by Orlando. In this environment, concentration of insect scatterers by the convergent winds along a gust front leading edge, combined with the formation of an "arcus" or "roll" cloud, result in moderately reflective thin line echoes that are readily recognizable in WSP base data.

Table 2.
Gust front detection and false-alarm probabilities by year.

	Orlando		Albuquerque
	'91	'92	'93
P_d	0.75	0.73	0.34
P_{fa}	0.0	0.13	0.06

In contrast, gust front radar cross-sections in Albuquerque were extremely low, owing to low relative humidity and significantly reduced insect scatterers. Typical thin-line echo magnitudes were 20 dB lower than in Orlando. Severe ground clutter in all quadrants surrounding the Albuquerque radar site further complicated detection of low cross-section gust fronts. The significant reduction in P_d for Albuquerque reflects primarily the lack of readily observable gust front signatures in WSP base data. Efforts underway to sensitize MIGFA, in combination with receiving chain modifications that will increase signal-to-noise at very close range should somewhat improve performance in this environment.

Performance of the storm motion algorithm has been quantitatively assessed by Chornoboy [8] on TDWR data from Denver and Kansas City. Errors in the estimates of storm advection speed and direction are related to the uncertainty in scan-to-scan displacements vectors. These in turn depend largely on the pixel size of the reflectivity images and the time interval between successive images that are cross-correlated. For the parameters used by the WSP, his analysis indicates that for storms moving faster than 10 kts, errors in the estimated direction of motion were less than 30^{o}; this error increases rapidly for storms moving more slowly. Mean error in the estimated speed of advection was 3 kts, independent of storm advection speed.

The performance of the anomalous propagation censoring function has been evaluated qualitatively in real time through operator comparison of WSP-generated reflectivity maps and coincident maps from the pencil-beam weather radars used as "truth." In addition, detailed comparisons have been conducted off line using recorded weather scenarios that vary from vigorous convection (air-mass and frontal thunderstorm systems) to widespread, stratiform rain. Overall these assessments indicate that the AP-censoring functioning is robust. Actual precipitation cells are rarely affected; exceptions have involved low-velocity, low reflectivity, stratiform rain. AP-induced ground clutter breakthrough is eliminated with high reliability. We have not observed significant instances where the censoring function failed to identify regions of false weather caused by AP.

C. Operational Evaluation of WSP Products

The WSP has been evaluated operationally each year since 1990 through display and utilization of its products in the ATC facilities at Orlando and Albuquerque. Following each year's evaluation, the FAA Technical Center (FAATC) distributed questionnaires to the controllers and supervisors who used the system to assess their perspectives on the strengths and weaknesses of the system.

Overall, Air Traffic Controller feedback on the WSP has been very positive. Over the four years of operational evaluation, from 80 to 100 percent of the respondents to the FAATC questionnaire have indicated that the WSP provides significant benefit to them in their job of controlling air traffic. The accuracy of the meteorological products was generally rated as "good" or "very good." Wind shear warnings from the system were routinely relayed by ATC to pilots and we noted a number of instances where the "planning products" (e.g., advance prediction of a gust front arrival at the airport) were used as an aid in air traffic management. During initial testing in Orlando, overly conservative warning criteria and buffer zones around detected microbursts resulted in situations where controllers felt the system sometimes impeded their ability to work aircraft in and around the weather. In response to their comments, modifications to the microburst algorithm were implemented that largely allayed such concerns. In Albuquerque, the low P_d for the very dry gust front/wind shift phenomena characteristic of that environment was cited as a problem, although

when provided, advanced warnings of gust front arrivals at the airport were viewed as very useful.

Individual Air Traffic Controller comments indicated that perceived benefits of the WSP lie in the areas of weather situational awareness and enhanced safety. The value of being able to anticipate weather impacts on flight routing and runway operations -- made possible by the GSD's broad-area, graphical depiction of relevant weather phenomena -- was emphasized in many of the comments. The capabilities to "provide estimates of when we would be able to resume arrivals and departures," "predict microburst impact [on runways] and plan accordingly," "predict [gust-front induced] runway changes" and "anticipate pilot requests for deviations" were examples of the benefits associated with the enhanced situational awareness provided by the WSP.

4. SUMMARY

Analysis and on-line testing of the prototype ASR-9 WSP has confirmed that the system can provide operationally beneficial detection of low-altitude wind shear phenomena and enhanced weather situational awareness for Air Traffic Control teams. As discussed, this dual-use capability for the ASR-9 has been achieved in the face of significant technical challenges. Innovative signal and image processing algorithms have been required to cope with the parameters of this aircraft detection and tracking radar. Algorithm refinement is ongoing, with emphasis on improved detection and prediction of wind shear phenomena in challenging environments such as the High Plains and Midwest U.S. Continued feedback will be obtained from operational testing with Air Traffic Controllers.

As of this writing, details of the FAA strategy for procurement of production WSP modifications for the ASR-9 are being addressed. Cost-benefit analyses have indicated that the system provides benefits -- in terms of reduced accident likelihood and enhanced air traffic planning capabilities -- that exceed its costs at approximately 50 airports that are not slated to receive a dedicated TDWR. A procurement plan is being developed that could result in national deployment of the system during the latter half of this decade.

REFERENCES

(1) M. Weber, M. Wolfson, D. Clark, S. Troxel, A. Madiwale, J. Andrews, "Weather Information Requirements for Terminal Air Traffic Control Automation," American Meteorological Society, Boston, Preprint Volume: *Fourth International Conference on Aviation Weather Systems,* Paris, France, June 24-28, 1991.

(2) E. Chornoboy, "Clutter Filter Design for Multiple-PRT Signals," American Meteorological Society, Boston, Preprint Volume: *26th International Conference on Radar Meteorology*, Norman, OK, May 24-28, 1993.

(3) M. Weber, "Ground Clutter Processing for Wind Measurements with Airport Surveillance Radars," Lexington, MA, Lincoln Laboratory Project Report ATC-143, FAA-PM-87-21, 4 November 1987.

(4) E. Chornoboy and M. Weber, "Variable PRF Processing for Meteorological Doppler Radar," IEEE National Radar Conference, March 29-31, 1994.

(5) M. Weber, "Dual-Beam Autocorrelation Based Wind Estimates from Airport Surveillance Radar Signals," Lincoln Laboratory Project Report ATC-167, FAA-PS-89-5, 12 June 1989.

(6) R. Delanoy and S. Troxel, "Machine Intelligent Gust Front Detection," Lexington, MA, Lincoln Laboratory Journal, Vol. 6, No. 1, Spring 1993, pp. 187-211.

(7) J. Verly, R. Delanoy and D. Dudgeon, "Machine Intelligent Technology for Automatic Target Recognition," Lexington, MA, Lincoln Laboratory Journal, Vol. 2, p. 277,1989.

(8) E. Chornoboy, "Storm Tracking for TDWR: A Correlation Algorithm Design and Evaluation," Lincoln Lexington, MA, Laboratory Project Report ATC-182, FAA-NR-91-8, 14 July 1992.